



## INVESTIGATING THE COMPRESSIVE TOE OF POST-TENSIONED CLT CORE-WALLS USING PARTICLE TRACKING TECHNOLOGY

J. Brown<sup>(1)</sup>, M. Li<sup>(2)</sup>, R. Nokes<sup>(3)</sup>, A. Palermo<sup>(4)</sup>, S. Pampanin<sup>(5)</sup>, F. Sarti<sup>(6)</sup>

<sup>(1)</sup> PhD Candidate, University of Canterbury, [justin.brown@pg.canterbury.ac.nz](mailto:justin.brown@pg.canterbury.ac.nz)

<sup>(2)</sup> Senior Lecturer, University of Canterbury, [minghao.li@canterbury.ac.nz](mailto:minghao.li@canterbury.ac.nz)

<sup>(3)</sup> Professor, University of Canterbury, [roger.nokes@canterbury.ac.nz](mailto:roger.nokes@canterbury.ac.nz)

<sup>(4)</sup> Professor, University of Canterbury, [alessandro.palermo@canterbury.ac.nz](mailto:alessandro.palermo@canterbury.ac.nz)

<sup>(5)</sup> Professor, Sapienza University of Roma, [stefano.pampanin@uniroma1.it](mailto:stefano.pampanin@uniroma1.it)

<sup>(6)</sup> Structural Engineer, PTL | Structural Consultants, [f.sarti@ptlnz.com](mailto:f.sarti@ptlnz.com)

### Abstract

Post-tensioned timber technology was originally developed and researched at the University of Canterbury (UC) in New Zealand in 2005. It can provide a low-damage seismic design solution for multi-storey mass timber buildings. Since mass timber products, such as cross-laminated timber (CLT), have high in-plane stiffness, a post-tensioned timber shear wall will deform mainly in a rocking mechanism. The moment capacity of the wall at the base is commonly determined using the elastic form of the Modified Monolithic Beam Analogy (MMBA). In the calculation of the moment capacity at the wall base, it is critical to accurately predict the location of the neutral axis and the timber compressive stress distribution.

Three 2/3 scale 8.6m tall post-tensioned CLT walls were experimentally tested under quasi-static cyclic loading – both uni-directional and bi-directional- in this study. These specimens included a single wall, a coupled wall, and a C-shaped core-wall. The main objective was to develop post-tensioned C-shaped timber core-walls for tall timber buildings with enhanced lateral strength and stiffness. To better understand the timber compressive stress distributions at the wall base, particle tracking technology (PTT) technology was applied for the first time to investigate the behaviour of the compression toe. Previous post-tensioned timber testing primarily used the displacement measurements to determine the timber compressive behavior at the wall base or rocking interfaces. However, by using PTT technology, the timber strain measurements in the compression zone can be much more accurate as PTT is able to track the movement of many particles on the timber surface.

This paper presents experimental testing results of post-tensioned CLT walls with a focus on capturing timber compressive behavior using PTT. The PTT measurements were able to better capture small base rotations which occurred at the onset of gap opening and capture unexpected phenomena in core-wall tests. The single wall test result herein presented indicates that while the MMBA could predict the moment rotation behavior with reasonable accuracy, the peak strain response was under predicted in the compression toe. Further detailed study is required to better understand the complex strain fields generated reflective of the inherent cross-thickness inhomogeneity and material variability of CLT.

*Keywords: post-tensioned timber; CLT; PTT; timber core-wall*



## 1 Introduction

Starting in 2005, post-tensioned timber technology, also called Pres-Lam, has been developed and researched at the University of Canterbury (UC) [1]. By adopting similar concepts and principles originally developed for precast concrete structures [2], it uses unbonded post-tensioned tendons to provide moment capacity at the wall base through clamping action. An extensive post-tensioned wall testing campaign with primarily laminated veneer lumber (LVL) at UC included single wall testing [1, 3], coupled wall testing with U-shaped flexural plates (UFPs) [4] and plywood [5], hybrid wall testing [6], and most recently a column-wall-column system [7]. While extensive work has been completed on post-tensioned in-plane wall systems, only preliminary studies on staircase cores [8] have verified the feasibility of post-tensioned core-walls. Outside of New Zealand, there has also been recent experimental testing of post-tensioned CLT in-plane shear walls by Ganey et al. [9] and a two-storey shake table test [10].

For design, a section analysis procedure similar to concrete has been outlined for the post-tensioned jointed ductile connection design of frame and wall structures [11]. Within this procedure, the elastic form of the Modified Monolithic Beam Analogy (MMBA), originally proposed by Pampanin et al. [12] and modified by Palermo [13], is used to calculate base moment and connection rotation at the rocking interface. Some distinct differences exist with timber to adopt this method from concrete. Material testing of LVL identified a suitable strain limit and the occurrence of an end-grain effect [14]. Investigation of the strain profile of the timber within the compression zone was performed and the linear profile was deemed suitable for design [15]. A detailed design guide has been published as a result of the research programme at UC [16].

In past research, the most common method for tracking the neutral axis depth at the base of a rocking timber wall is to linearly interpolate a number of single point measurements by Linear Variable Displacement Transducers (LVDTs). If a detailed analysis of the rocking interface is desired, Particle Tracking Technology (PTT) has advantages over traditional LVDTs as the movement of a large number of particles can be tracked with digital cameras with high resolution.

Particle Tracking Technology (PTT) is a contact-free quantitative field measuring technique originally developed to track individual particles in fluid flows [17]. The use of PTT has gained popularity in the structural space as displacement and strain fields can be generated while traditional LVDTs and strain gauges only provide one measurement per device. Within structural timber testing, Ottenhaus et al. [18] have shown the versatility of PTT with CLT testing in dowel embedment tests, large scale CLT connection tests and small scale material tests. It was shown that PTT could successfully capture displacements with increased accuracy to LVDTs, capture unexpected movements, and additionally capture strain fields. The system used to process the images and implement PTT algorithms was Streams [17], which is software originally developed at the University of Canterbury for the field of fluid mechanics.

This paper presents the use of PTT for the first time in post-tensioned CLT structural testing. With PTT, the neutral axis depth and strains at the rocking interface can be determined. Single and coupled wall testing results will be used to compare with analytical predictions. While a post-tensioned CLT core-wall introduces increased complexity with multiple potential rocking surfaces, the displaced shape of the compression toe and out-of-plane flange behaviour captured with PTT will be presented. In the cases of open floor plans or taller timber buildings, a post-tensioned C-shaped core-wall with proper connection detailing can provide enhanced lateral strength and stiffness.

## 2 Post-tensioned CLT Core-wall Experimental Setup

The experimental programme consisted of quasi-static cyclic testing under either uni-directional [19] and/or bi-directional cloverleaf loading for three post-tensioned CLT shear wall specimens: a single wall in test Phase I, a coupled wall in test Phase II, and a C-shaped core-wall in test Phase III. The wall specimens were 8.6m and four storeys high with a 2/3 scale factor. The lengths of the web walls (Wall 1 and Wall 2) were 1912mm and those of the flange walls (Wall 3 and Wall 4) were 1450mm. The CLT wall panels were 5-ply and 175mm thick (45/20/45/20/45) with SG8 Douglas-fir laminations as specified in NZS3603:1993 [20]. CLT floors at



each of the four levels provided required lateral restraint. Some distinct material differences between LVL used in past testing by Sarti et al. [6] and CLT in this testing campaign are shown in Table 1. The  $E$ ,  $f_{c,0}$ ,  $f_{c,90}$ , and lamella thickness,  $t$ , will all influence the behaviour of the rocking interface at the compression toe.

Table 1: LVL and CLT material properties

Material	Modulus of Elasticity, $E$ (MPa)	Compression strength (MPa)		Veneer / lamella thickness, $t$ (mm)
		Parallel to grain, $f_{c,0}$	Perpendicular to grain, $f_{c,90}$	
LVL [21]	11 000	45	n/a	2.5 - 5.0
CLT [22]	8 000	18	8.9	20.0 - 45mm

At the CLT wall base, EA 125x125x12 [23] shear keys provided in-plane and out-of-plane restraint. For some tests, UFP dissipaters were installed at the corner and base of each CLT wall to provide additional energy dissipation. A total of twelve  $\phi 26.5$ mm Macalloy bars [24] anchored the four CLT wall components to the foundation. The Macalloy bars were located within 100 x 45mm voids in the middle layer of the CLT, and secured to the top of each CLT wall with a 50mm thick steel anchorage plate. A more detailed explanation on the experimental test set-up, programme and methodology can be found in Li & Brown [25]. The test setup and the configuration of the Phase III C-shaped core-wall are shown in Fig. 1 and Fig. 2 respectively.



Fig. 1 - C-shaped core-wall specimen

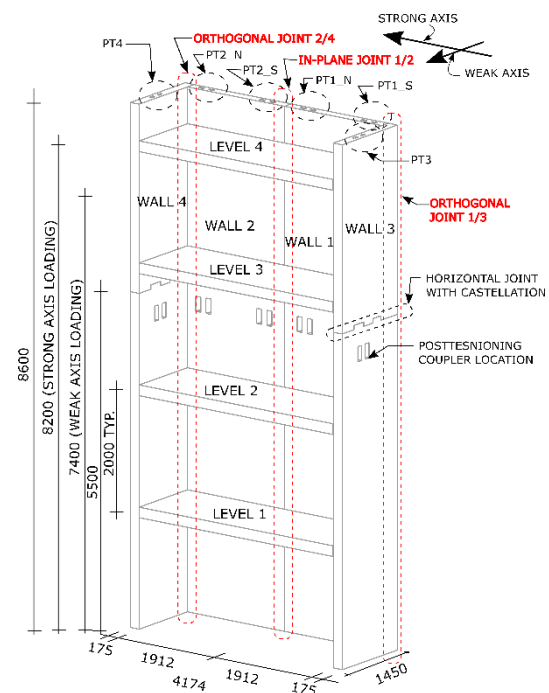


Fig. 2 - Core-wall specimen isometric

### 3 Test Programme and Methodology

The post-tensioned CLT wall programme is shown in Fig. 3. A total of 17 tests were performed: five tests in Phase I, five tests in Phase II and seven tests in Phase III. By testing three different shear wall configurations, the enhanced lateral strength and stiffness could be directly assessed. In Phase II and III, different screwed connection details between the CLT wall panels provided the enhanced stiffness and strength through composite action. The screws were installed at 90°, inclined or mixed angles with each providing different connection strength, stiffness and displacement capacity as reported by Brown & Li [26]. The different screwed connections used are shown in Fig. 4. The uni-directional quasi-static displacement controlled loading protocol followed ACI ITG-5.1-07 [19]. For some tests, a cloverleaf bi-directional loading



protocol was followed. Fig. 2 shows the lateral loads applied along the strong axis at one point aligned with the web walls and along the weak axis at one point for each flange wall. In this paper, one single wall, one coupled wall, and two core-wall tests are discussed in relation with PTT at the wall base. Table 2 provides some details of the four tests.

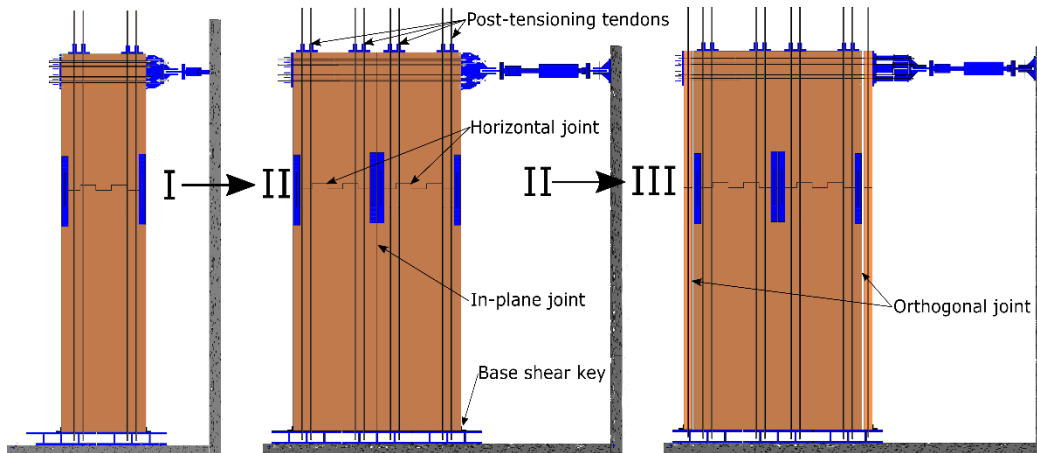


Fig. 3 - Post-tensioned CLT wall testing programme

Table 2 - Summary of chosen CLT shear wall tests

Test	In-plane joint	Orthogonal joint	Max. drift (%)
I-2	n/a	n/a	0.9
II-3	90 degree screws	n/a	1.2
III-2	90 degree screws	90 degree screws	1.5
III-6	Mixed angle screws	Mixed angle screws	2.3

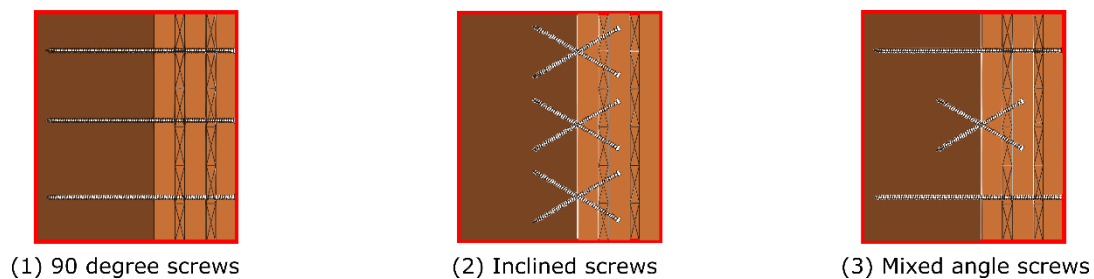


Fig. 4 - Orthogonal joint screwed connection options

In total, 220 LVDTs, 16 load cells, and 20 inclinometers were installed to measure the wall response. LVDTs monitored in-plane and out-of-plane movement, neutral axis location at the core-wall base, core-wall sliding, relative slip between CLT walls, castellation movement, diaphragm movement and UFP connection movement. Load cells monitored each actuator and post-tensioning bar, and inclinometers recorded wall and floor rotations. At the shear wall base both LVDTs and PTT were implemented.

### 3.1 PTT Setup and Processing

PTT was implemented at the base of each CLT wall to better understand the base rocking interface. The methodology used in the testing was adopted from previous work by Ottenhaus et. al. [18]. For the experimental set-up, ten Fujifilm X-T2 cameras with XF 18-55 lens were positioned around the core-wall base on stiff supports. The resolution of the images was 6000x4000 pixels, and the PTT resolution ranged from



0.145 mm/pix to 0.197 mm/pix. Artificial lighting was provided to ensure a consistent light intensity throughout each image frame. For particles, 8mm diameter blue circle stickers were attached to the CLT wall surface. As particles were placed on the face of the CLT wall, all displacement and strains recorded represent surface values. An image was recorded at each displacement step of the loading protocol such that each image could easily be correlated with the associated experimental data file. Fig. 5 shows the PTT setup at the core-wall base and an image view of one camera.

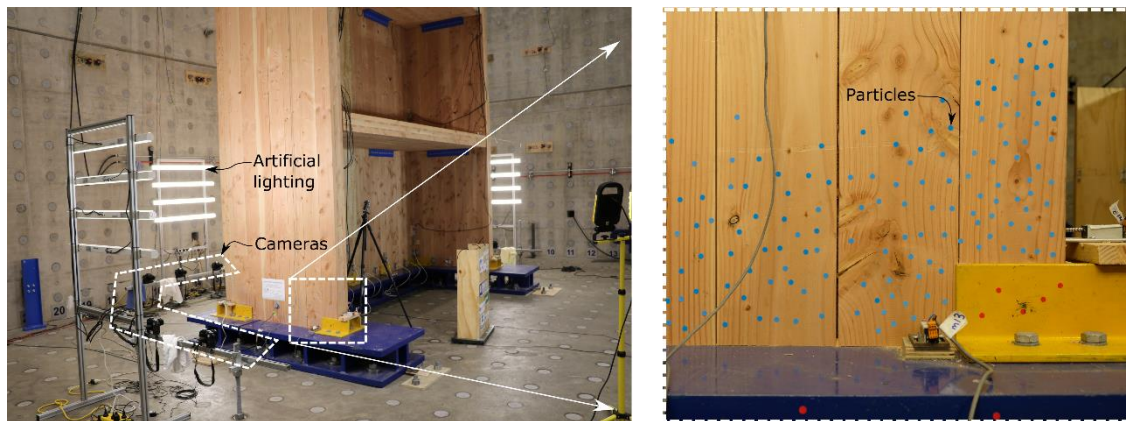


Fig. 5 - PTT setup at core-wall base: general setup with image from a single camera

Streams [17] was used in image post processing and it has an extensive toolkit of processes to perform image filtering, particle identification, PTT analysis, and ultimately produce displacement and strain fields. The particle identification algorithms within Streams require the ability to identify and distinguish the pixels that comprise the particles and differentiate them from the rest of the image frame. This is accomplished by a variation in light intensity on either a grey or RGB scale.

In the following, the processes performed to analyse this particular image set will be described with reference to Fig. 6. The images were pre-processed and filtered by subtracting the red intensity from the blue. This accentuated the blue particles against the natural timber background. Particles were then identified as comprising the pixels whose blue intensity exceeded a user defined threshold. The two particles shown in Fig. 6c moved vertically approximately 30mm in this test. For Test III-6, 7850 images were processed for each of the ten cameras around the wall base.

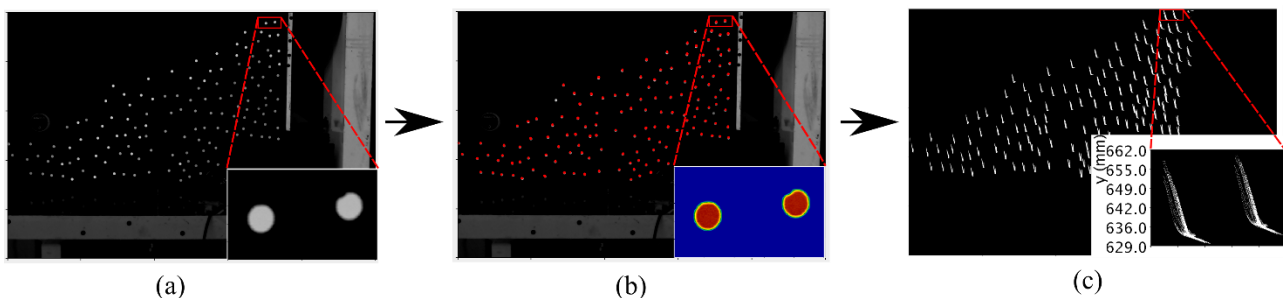


Fig. 6 - Particle identification: (a) Image filtering, (b) particle identification, (c) particle path

In order to track the particles between each image frame, each particle in the image frame must be matched with particles in the next frame. Streams used an optimisation process based on finding the particle in the next frame that is closest to the particle in the first frame. The collection of all distinct particles paths comprise the particle record. Particle records were combined together as required such that a displacement or strain field for a Phase I single wall (three cameras), Phase II coupled wall (six cameras) or Phase III core-wall (ten cameras) could be interpreted together.

With particle records, Streams generated a material displacement field on a rectangular grid corresponding to  $x$ ,  $y$ , and  $t$  (the time of each image). Particle displacements were interpolated onto the grid



using a standard triangulation method similar to that used in finite element analysis. Displacements were transformed into a material-based frame of reference such that displacements and strains were computed relative to the wall before testing began.

#### 4 Post-tensioned CLT Core-wall Test Programme Results

The global force-drift curves for the four chosen tests are shown in Fig.7. For Tests I-2, II-4 and III-2 the wall drifts were limited to minimize damage at the compression toe. For Test III-6 wall drift was limited by ram stroke. A typical nonlinear elastic behaviour was observed in all tests, with the onset of gap opening at the base of the wall coinciding with the change in stiffness of the force drift curves. There is a significant change in stiffness and strength when comparing a Phase I single wall, Phase II coupled wall, and Phase III core-wall system. A detailed discussion on the key post-tensioned wall results can be found in a different publication [25]. The core-wall test results of Tests III-2 and III-6 indicate that the composite action achieved is a function of the connection detail chosen between the panels, and especially between flange and web walls. The connection provides the necessary strength to engage the tension flange and its post-tensioning bars in uplift and to distribute compressive strains to the compression toe. By using PTT, we can more accurately track the displacement and strain fields at the compression toe to quantify this engagement.

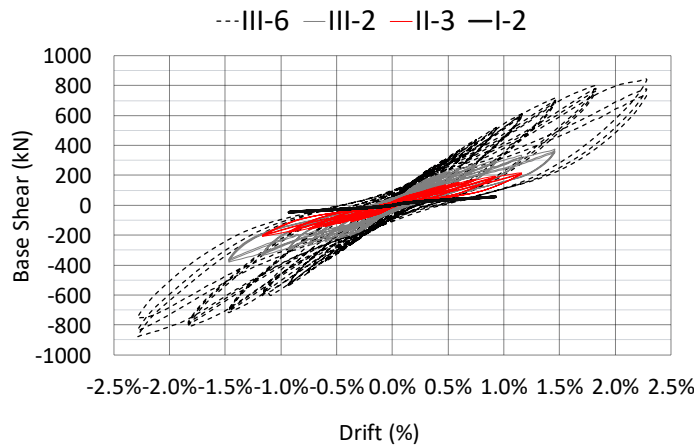


Fig.7 - Global hysteresis curves for selected tests

Fig. 8 and Fig.9 show 2mm and 12mm residual deformations in Wall 2 due to non-recoverable wood crushing after test Phase II and III respectively. Fig.14 indicates the peak strain level recorded in Test II-3.

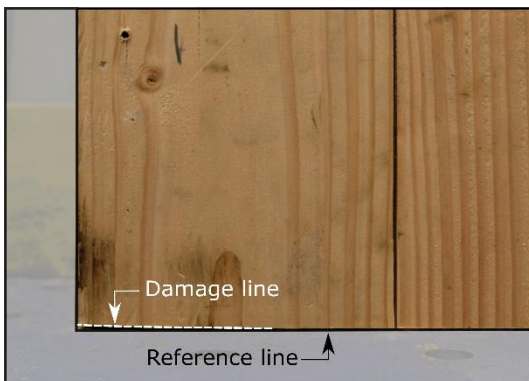


Fig. 8 - Wall 2 toe after Phase II

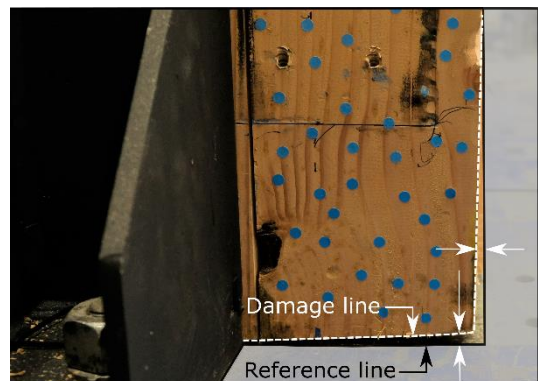


Fig.9 - Wall 2 toe after Phase III



## 5 PTT Results and Discussion

The accuracy of PTT can be first verified by comparing the PTT readings with LVDTs for the Phase I single wall test. In Phase I and II, the general displacement and strain behaviour will be presented and in Phase III, the engagement of the flange wall based on PTT will be shown. The results presented with PTT indicate displacement and strain at the CLT surface. The inherent material inhomogeneity and cross-thickness variation of CLT introduce complexities for future detailed analysis and verification with comparison to the MMBA.

### 5.1 Comparison to LVDT and MMBA / Compression toe distribution along wall base

A comparison of the neutral axis depth from analytical predictions with the MMBA and Test I-2 using LVDTs and PTT is shown in Fig.10. In general, the LVDT and PTT measurements agreed, and the MMBA predicted depth of neutral axis was greater than the test results. With LVDTs, the neutral axis location was determined by using a linear function to fit the seven spring loaded LVDT readings at the base of each wall. If one LVDT stopped recording properly, or if the timber that the LVDT was fastened to crushes as shown in Fig.11, the accuracy of the linear fit function would decrease. This relatively small number of measuring points to fit a linear trend accounts for differences between LVDT and PTT results even at larger rotations. With PTT, more than 300 particles were tracked on each wall to create a displacement field. In Fig.10, a more smooth transition at small connection rotations indicates that the neutral axis depth was better determined by PTT than LVDTs.

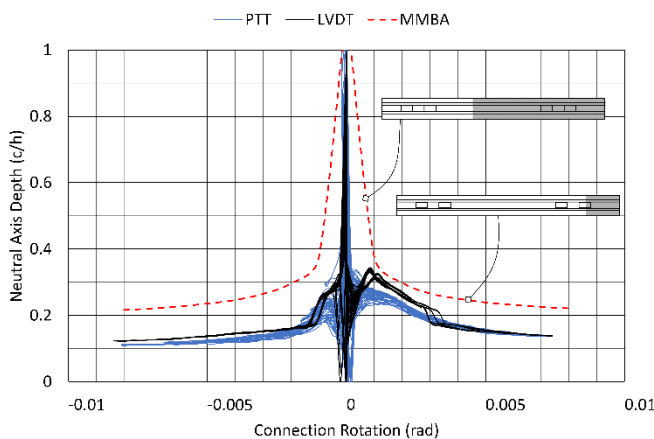


Fig.10 - Test I-2 - Neutral axis depth comparison



Fig.11 - Wall 2 compression failure at LVDT

In Fig.12, the Test I-2 displacement and strain field, generated with PTT, is compared with MMBA predictions for a wall drift of 0.9%.  $Y_c$  represents vertical movement, and  $x$  and  $y$  represent the material location along the wall with respect to its lower corner. At 0.9% drift, the MMBA is over predicting the neutral axis depth, and thus under predicting the peak strain level. The MMBA prediction and experimental neutral axis are 325mm and 150mm respectively. The experimental results indicate that there was an initial disturbed region near the location of the neutral axis, and that throughout the neutral axis depth the strain field is quite variable with a distinct trend hard to discern. It is worth noting that although the MMBA is over predicting the neutral axis, the global system response is reasonably well predicted and within 15% when characteristic material properties are used and only parallel-to-grain CLT layers are considered [25].

As stated above, LVL is a relatively more homogenous material when compared to CLT, and past research has primarily used LVL with the MMBA to predict the response. Fig.12 shows two different neutral axis and strain predictions when the effective elastic modulus and wall width are varied within the MMBA calculation. With CLT, the impact of the cross-layer, the higher probability of imperfections due to knots and checks near the compression toe, and the fabrication process including being non-edge glued panels all add to the variability in strain that is reflected in Fig.12. This is significantly different than LVL, where thin lamella are glued together such that all fibres are aligned and the influence of knots and checks are almost eliminated.

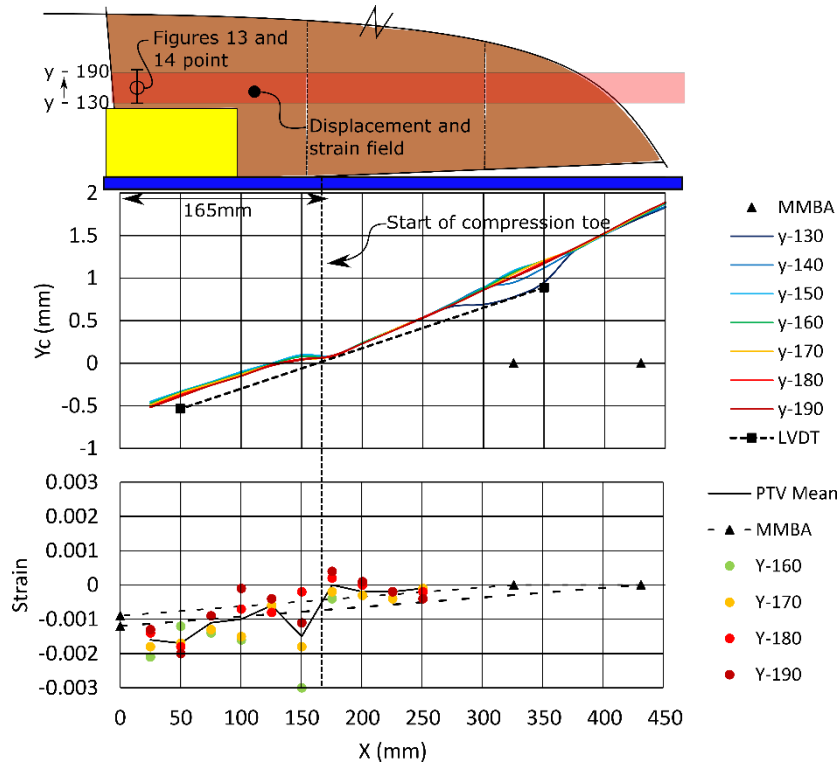


Fig.12 - Test I-2- Displacement and strain distribution with comparison to MMBA

**5.2 Displacement and strain fields at compression toe**

The displacement and strain at a point near the shear wall toe for Test I-2 and Test II-3 respectively is shown in Fig.13 and Fig.14. In these figures *t* represents a position on the loading cycle. Refer to Fig.12 for the point location. The vertical displacement change from *y*=130 to *y*=200 during rocking to the toe indicates compression, which is reflected as compressive strain. The maximum compressive strain recorded was -1800 and -3000  $\mu\epsilon$  for Test I-2 and II-3 respectively. In Fig.14, the three cycles at 1.2% drift are presented with compression strain occurring when the point is within the neutral axis and tension strain occurring during uplift. Though the measured strain of Test II-3 was beyond the characteristic elastic strain value, a linearly increasing compression strain trend to peak 1.2% wall drift at *t*=67.0, 72.5, and 78.0 was observed. This indicates that stable behaviour beyond the characteristic elastic strain occurred at the point indicated in Fig.12.

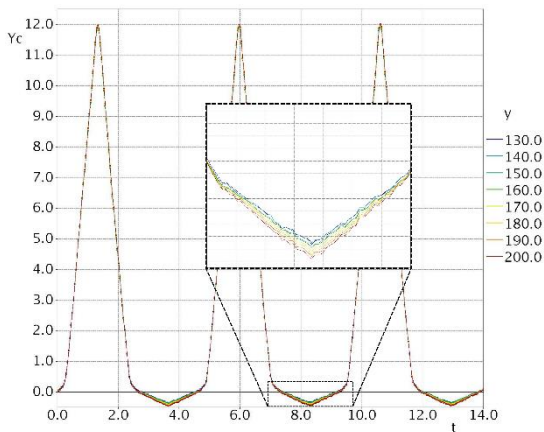


Fig.13 - Test I-2 displacement at 0.9% drift

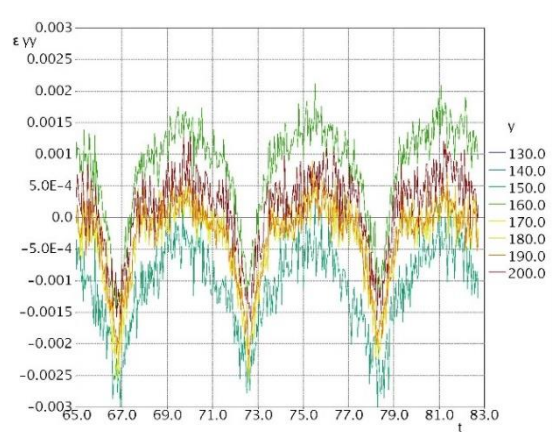


Fig.14 - Test II-3 strain at 1.2% drift



The displacement field at peak drift is shown for Test II-3 and III-2 respectively in Fig. 15 and Fig. 16. These displacement fields are generated from PTT. Agreeing with the single wall Test I-2, there is a distinct disturbed region shown at  $x=1550\text{mm}$  in Fig. 15 where more significant compression occurs. Following the disturbed region, the displacements over 250mm wall height,  $y$ , change in a relatively similar manner.

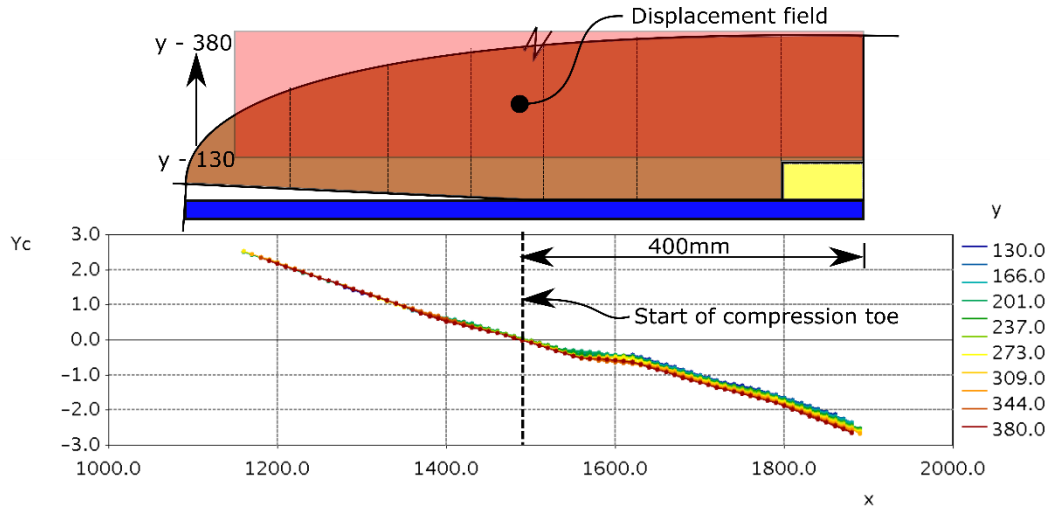


Fig. 15 - Test II-3 compression toe displacement at 1.2% drift

Fig. 16 shows that for a core-wall, the flange engagement lessens with increasing distance from the corner as expected.

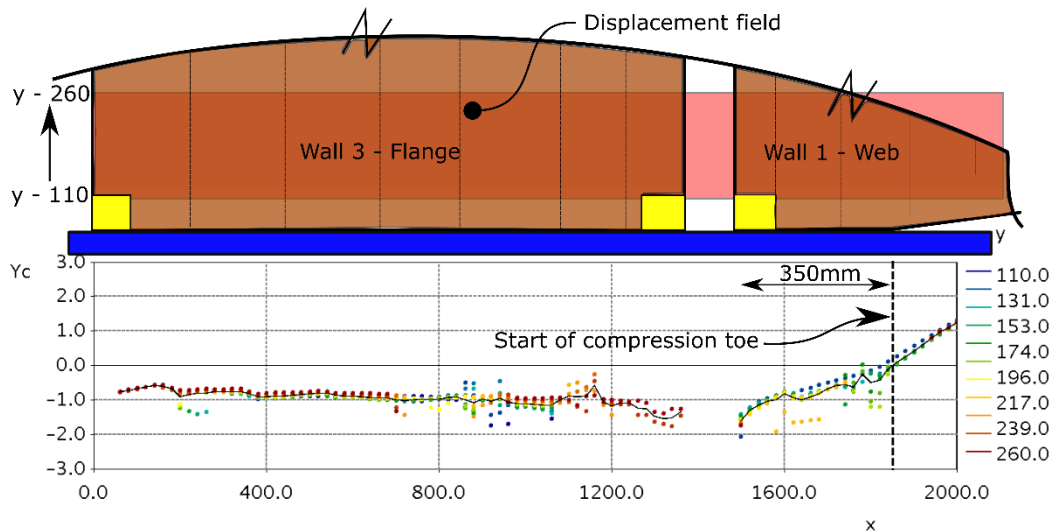


Fig. 16 - Test III-2 compression toe displacement at 1.5% drift

### 5.3 Core-wall tests out-of-plane behaviour

The behaviour of the compression toe during core-wall testing is more complex than traditional in-plane shear wall systems. The unsymmetrical behaviour of the C-shaped core-wall causes twist during strong axis loading, and the ability to transfer compressive forces created from tension in the post-tensioning bars is determined based on the connection details between the CLT wall panels. Preliminary results of Test III-2 which used 90 degree screws and Test III-6 which used mixed angle screws are presented.



Fig.17 shows that during strong axis loading, significant and unexpected out-of-plane rotation occurred in the flange wall during Test III-2. At 1.5% drift, less than one third, approximately 50mm, of the flange wall was in contact with the foundation. However, in Test III-6 at both 1.5% and 2.3% drift the entire flange was in contact with the foundation.

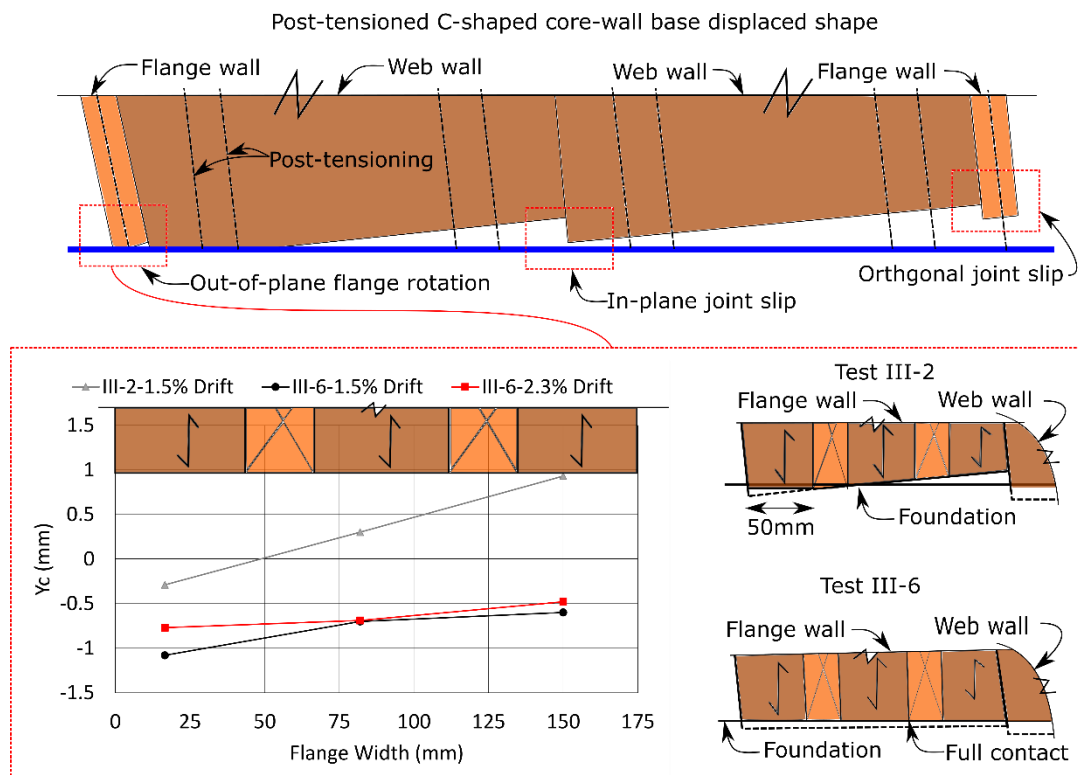


Fig.17 - Core-wall out-of-plane behaviour

The relatively less stiff screwed connection between the web and flange wall of Test III-2 could not restrain the out-of-plane rotation. The use of PTT allowed for this unexpected phenomena to be captured and recorded. If a core-wall were designed with the same screwed connection details of Test III-2, only 50mm of the flange could be accounted for in compression with section analysis at the wall base.

## 6 Conclusions

This paper presented for the first time the use of PTT in post-tensioned timber shear wall testing of single wall, coupled wall and core-wall configurations to create a displacement and strain field at the wall base. The accuracy of PTT to predict the neutral axis was verified in comparison with the LVDT measurements, and it was shown to better capture small base rotations which occurred at the onset of gap opening. PTT was able to capture the unexpected significant out-of-plane rotations of the flange walls during core-wall Test III-2. This phenomenon would have been difficult to measure with traditional LVDTs.

While Test I-2 results indicated that the MMBA could under-predict the peak strain response in the compression toe, further detailed study is required. The complex strain fields generated in each test are reflective of inherent cross-thickness inhomogeneity and the increased material variability of CLT when compared to LVL. The disturbed region observed in each test indicated that the strain distribution might not be exactly linear for post-tensioned CLT rocking walls. However, at the system level the linear strain distribution assumption in the MMBA is still able to predict the moment rotation behaviour with reasonable accuracy. The results of Test II-3 also showed that stable system behaviour occurred when the measured timber strains were beyond the elastic limit. However, current analytical prediction methods for post-tensioned CLT walls may lead to an underestimation of the peak timber strain, thus leading to a slight overdesign of the



reinforcement and reduction of the actual drift and strain level in the timber. Yet, should the target drift be reached at a higher intensity level, the predictive relationship between drift and local strain might lead to an underestimation of the local timber compression damage. Therefore, further investigation with PTT and CLT post-tensioned walls with different post-tensioning levels is needed to better define the compressive stress distribution at the wall base.

## 7 Acknowledgements

This research programme was made possible through the sponsorship of Speciality Wood Products Partnership, New Zealand Douglas-Fir Association, Australian Research Council, SPAX Pacific, BBR Contech and the New Zealand Commonwealth Scholarship and Fellowship Plan. The technical comments from Dr. Lisa Ottenhaus regarding PTT and technical support from University of Canterbury technicians Peter Coursey, Russell McConchie, Alan Thirwell and Michael Weavers are gratefully acknowledged. PTL | Structural Consultants is acknowledged for the use of the Pres-Lam system in this research.

## 8 References

- [1] A. Palermo, S. Pampanin, A. H. Buchanan, and M. P. Newcombe, "Seismic design of multi-storey buildings using laminated veneer lumber (LVL)," in *New Zealand Society for Earthquake Engineering Conference*, 2005, no. 14, p. 8.
- [2] M. J. N. Priestley, "Overview of PRESSS research program," *PCI J.*, vol. 36, no. 4, pp. 50–57, 1991.
- [3] A. Palermo, S. Pampanin, and A. H. Buchanan, "Experimental investigations on LVL seismic resistant wall and frame subassemblies," in *European Conference in Earthquake Engineering and Seismology (ECEES)*, 2006.
- [4] A. Iqbal, S. Pampanin, A. Palermo, and A. H. Buchanan, "Performance and Design of LVL Walls Coupled with UFP Dissipaters," *J. Earthq. Eng.*, vol. 19, no. 3, pp. 383–409, 2015.
- [5] A. Iqbal, T. Smith, S. Pampanin, M. Fragiaco, A. Palermo, and A. H. Buchanan, "Experimental performance and structural analysis of plywood-coupled LVL walls," *J. Struct. Eng.*, vol. 142, no. 2, 2015.
- [6] F. Sarti, A. Palermo, and S. Pampanin, "Quasi-Static Cyclic Testing of Two-Thirds Scale Unbonded Posttensioned Rocking Dissipative Timber Walls," *J. Struct. Eng.*, vol. 142, no. 4, pp. 1–14, 2016.
- [7] F. Sarti, A. Palermo, and S. Pampanin, "Development and testing of an alternative dissipative post-tensioned rocking timber wall with boundary columns," 2016.
- [8] A. J. M. Dunbar, "Seismic design of core-wall systems for multi-storey timber buildings," University of Canterbury, Christchurch, N.Z, 2014.
- [9] R. Ganey *et al.*, "Experimental Investigation of Self-Centering Cross-Laminated Timber Walls," *J. Struct. Eng.*, vol. 143, no. 10, 2017.
- [10] S. Pei *et al.*, "Experimental Seismic Response of a Resilient 2-Story Mass-Timber Building with Post-Tensioned Rocking Walls," *J. Struct. Eng.*, vol. 145, no. 11, pp. 1–15, 2019.
- [11] M. P. Newcombe, S. Pampanin, A. Buchanan, and A. Palermo, "Section analysis and cyclic behavior of post-tensioned jointed ductile connections for multi-story timber buildings," *J. Earthq. Eng.*, vol. 12, pp. 83–110, 2008.
- [12] S. Pampanin, M. J. Nigel Priestley, and S. Sritharan, "Analytical modelling of the seismic behaviour of precast concrete frames designed with ductile connections," *J. Earthq. Eng.*, vol. 5, no. 3, pp. 329–367, 2001.
- [13] A. Palermo, "Use of controlled rocking in the seismic design of bridges," Technical Institute of Milan, Milan, Italy, 2004.
- [14] M. P. Newcombe, "Seismic design of multistorey post-tensioned timber buildings," University of Pavia, Pavia, Italy, 2008.
- [15] T. Smith *et al.*, "Seismic response of hybrid-LVL coupled walls under quasi-static and pseudo-dynamic testing," in *2007 New Zealand Society for Earthquake Engineering Conference, Palmerston North, New Zealand*, 2007, vol. 8.



- [16] S. Pampanin, A. Palermo, and A. Buchanan, *Post-Tensioned Timber Buildings - Design Guide Australia and New Zealand*. Christchurch: Structural Timber Innovation Company, 2013.
- [17] R. Nokes, *Streams 3.02: System Theory and Design*. 2019.
- [18] L.-M. Ottenhaus, M. Li, R. Nokes, P. Cammock, and B. McInnes, "Use of particle tracking velocimetry in timber material and connection testing," *Eur. J. Wood Wood Prod.*, vol. 77, no. 2, pp. 195–209, 2019.
- [19] ACI Innovation Task Group 5, "Acceptance criteria for special unbonded post-tensioned precast structural walls based on validation testing and commentary : an ACI standard." American Concrete Institute, Farmington Hills, MI, 2008.
- [20] Standards New Zealand, *Timber structures standard*, NZS 3603., no. 1. Wellington, New Zealand, 1993.
- [21] Nelson Pine Industries Ltd., *Nelson Pine LVL. Specific engineering design guide*. Nelson, New Zealand, 2016.
- [22] XLam NZ Limited, *XLam design guide*. Nelson, New Zealand, 2017.
- [23] Australian / New Zealand Standard and A. 3679.1:2016, "Steel reinforcing materials," 2016.
- [24] Macalloy, "European organization for technical approval ETA-07/0046," Charlottenlund, Denmark, 2007.
- [25] M. Li and J. Brown, "SWP-T082: Experimental studies on Douglas-fir CLT connections and core-walls," Christchurch, N.Z, 2019.
- [26] J. Brown and M. Li, "Behaviour of Screwed Connection Installed with Mixed Angles between Orthogonal CLT Plates (submitted)," in *New Zealand Society for Earthquake Engineering Conference*, 2020.